Available online at www.sciencedirect.com
SCIENCE DIRECT®
Journal of Sound and Vibration 272 (2004) 675–701
JOURNAL OF SOUND AND VIBRATION
www.elsevier.com/locate/jsvi

Multiple time scale analysis of hysteretic systems subjected to harmonic excitation

Nobukatsu Okuizumi[a,*], Koji Kimura[b]

[a] *Space Structures Laboratory, The Institute of Space and Astronautical Science, 3-1-1 Yoshinodai, Sagamihara, Kanagawa 229-8510, Japan*

[b] *Department of Mechanical and Environmental Informatics, Tokyo Institute of Technology, 2-12-1 Ookayama, Meguro-ku, Tokyo 152-8552, Japan*

Received 23 November 2001; accepted 11 April 2003

Abstract

Dynamic behavior of smooth hysteretic systems subjected to harmonic excitation is analyzed. Wen's differential equation model for hysteresis, which can be applied to a large class of hysteretic systems, is used. A piecewise power series expression for hysteretic restoring force is derived from Wen's model assuming that steady state force–displacement curve draws a single loop and that the non-linearity of the restoring force is weak. The method of multiple scales is applied to the equation of motion by using the piecewise power series expression for the cases of primary and secondary resonance to derive the approximate solutions and the differential equations governing the amplitude and phase of the solutions. Phase plane trajectories, resonance curves and stability limit of the solutions are obtained and compared with the results of numerical integration in order to examine the validity of the present analysis.

1. Introduction

Many mechanical and structural systems subjected to severe dynamic loads exhibit hysteretic behavior. In such systems, the restoring force depends on their past histories and the force–displacement relationships are not single-valued and draw hysteretic loops. Due to this nature, hysteretic systems may display complex dynamic behavior and have energy dissipation properties. Investigating the vibration characteristics of hysteretic systems is important for the reliability and safety of mechanical and structural systems.

*Corresponding author: Fax: +81-42-759-8297.
E-mail address: okuizumi@pub.isas.ac.jp (N. Okuizumi).

0022-460X/03/$ - see front matter © 2003 Elsevier Ltd. All rights reserved.
doi:10.1016/S0022-460X(03)00404-8

Recently, bifurcation and chaos in non-linear vibrating systems have drawn much attention. They have been extensively investigated by using various analytical methods and a vast amount of knowledge has been obtained for elastic systems. However, these phenomena of hysteretic systems have not been studied as much as elastic systems in spite of their importance.

This is mainly because the restoring force has a multi-valued nature so that approximate analytical techniques, which are useful for non-linear elastic systems, cannot be applied directly to hysteretic systems except for the first order averaging method. Most of the studies from the viewpoint of non-linear dynamics have been restricted for the case of specific external forcing or specific softening or hardening systems [1–3].

In the former studies of non-linear vibration of hysteretic systems, Caughey applied the method of slowly varying parameters, i.e., the first order averaging method to a single-degree-of-freedom (s.d.o.f.) bilinear hysteretic system subjected to harmonic excitation and obtained the approximate solution and its stability [4]. His method has been frequently used for various hysteretic systems under harmonic excitations, such as s.d.o.f. smooth softening systems [5,6], piecewise-linear systems [6–8], degrading piecewise-linear systems [6,9], degrading smooth softening system [6], two-d.o.f. bilinear system [10], double pendulum with bilinear hysteretic damping [11] and so on. Caughey's method is useful for obtaining the first order approximate solutions for the case of primary resonance while his method cannot be readily applicable to the higher order solutions. Concerning higher order approximate analysis, numerical procedures based on the method of harmonic balance [12] were employed for smooth hysteretic systems [2,13]. The method of multiple time scales [14] and higher order averaging method [15], which are useful for stability and bifurcation analyses of weakly non-linear elastic systems, have seldom been applied to hysteretic systems.

From the viewpoint of non-linear dynamical system, Poddar et al. [16] investigated the vibrations of an elasto-plastic beam, the Shanley model, under periodic impulse forcing and numerically confirmed the existence of chaotic motion. Pratap et al. [17,18] analyzed the free and forced oscillations of a bilinear hysteretic system, which was a simplification of the Shanley model, under parametric periodic impulse forcing. They revealed that there exist numerous bifurcations from quasi-periodic motion to chaos-like motion. Pratap and Holmes [1] studied the behavior of a piecewise linear map which describes the motion of the same bilinear oscillator under parametric impulse forcing and proved that chaotic motion in the form of a Smale horseshoe [19,20] exists. Capecchi et al. [9] showed the existence of not only jump phenomena but also Hopf bifurcation [19,20] in a degrading piecewise linear hysteretic system by applying Caughey's method. He also applied a numerical procedure based on the method of harmonic balance to a smooth softening degrading hysteretic system and showed that the periodic solution became unstable via Hopf bifurcation and suggested that chaotic motion might appear [2]. Yang et al. [3] investigated a smooth hysteretic system using a model of Baber and Wen [21] by numerical integration and demonstrated the occurrence of the chaotic vibration for the case of hardening hysteretic system under cyclic loading of large amplitude.

In this paper, we investigate smooth hysteretic systems by using the method of multiple time scales for the cases of primary and secondary resonance. Wen's differential equation model [22], which can describe a large class of hysteretic systems is used. In order to apply the method of multiple time scales, a piecewise power series expression for hysteretic restoring force is proposed. By using this expression, the method of multiple time scales is applied up to the second order and

the symmetric approximate solutions and differential equations describing the modulations of the amplitudes of the solutions are obtained. For the case of primary resonance, phase plane trajectories and resonance curves of the solutions are obtained. For the case of secondary resonance, the phase plane trajectories and unstable regions of symmetric solutions are obtained. It is shown that the symmetric solutions become unstable and non-symmetric solutions diverge in the secondary resonance region via pitchfork bifurcation [19,20]. Analytical results are compared with the results of numerical integration of Wen's model in order to determine the validity of the present analysis.

2. Model for hysteresis

The equation of motion for a s.d.o.f. hysteretic system subjected to harmonic excitation is of the form

$$\ddot{x} + \bar{\delta}\dot{x} + kx + z = \bar{f}\cos\omega t, \tag{1}$$

where x is the displacement, z is the hysteretic restoring force, $\bar{\delta}$ is the damping coefficient, k is the linear stiffness coefficient, $\bar{f}$ and ω are the amplitude and frequency of external forcing, respectively. Using Wen's differential equation [22], a model for hysteretic restoring force can be constructed by requiring x and z to satisfy the following differential equation:

$$\dot{z} = A\dot{x} - (\bar{\beta}|\dot{x}||z|^{n-1}z + \bar{\gamma}\dot{x}|z|^{n}), \tag{2}$$

where A, $\bar{\beta}$ and $\bar{\gamma}$ are the parameters to control the scale and general shape of the hysteretic loop, while n controls the smoothness of the loop. By adjusting the values of $\bar{\beta}$ and $\bar{\gamma}$, a wide variety of smooth restoring forces, such as softening or hardening, narrow or wide loops is described. Depending on whether $\bar{\beta} + \bar{\gamma}$ is positive or not, this system exhibits softening or hardening hysteretic characteristics, respectively. As $\bar{\beta}$ increases, the width of the hysteretic loop, i.e., the dissipation energy due to hysteresis becomes large.

In this paper, we set $n = 1$ and consider the case of exponential hysteretic restoring force. Then the equations of motion for the present hysteretic system are the following system of differential equations:

$$\begin{aligned} &\ddot{x} + \bar{\delta}\dot{x} + kx + z = \bar{f}\cos\omega t, \\ &\dot{z} = A\dot{x} - (\bar{\beta}|\dot{x}|z + \bar{\gamma}\dot{x}|z|). \end{aligned} \tag{3}$$

3. The piecewise power series expression for hysteretic restoring force

Equations of motion (3) for the present system have three state variables: $x, \dot{x}$ and z. The restoring force z is not expressed by the polynomial of the displacement x. Therefore typical approximate analytical methods to non-linear vibrating systems, such as the averaging method or the method of multiple time scales, cannot be applied directly to Eq. (3). In order to use these methods, the piecewise power series expression for hysteretic restoring force is proposed.

3.1. Division of hysteretic loop

As shown in Fig. 1(a), we assume that force–displacement curve draws a single loop in stationary state. The case of double loops (Fig. 1(b)) or more is beyond the scope of this paper. Depending on the signs of velocity $\dot{x}$ and hysteretic restoring force z, the hysteretic loop can be divided into four intervals. In each interval, Eq. (3) is integrated and z is described by the following equations.

Interval(i): $\dot{x} \leqslant 0,\ z \geqslant 0$

$$z = \begin{cases} -\dfrac{A - B_1 e^{(\bar{\beta}-\bar{\gamma})x}}{\bar{\beta}-\bar{\gamma}} & (\bar{\beta}-\bar{\gamma} \neq 0), \\ Ax + D_1 & (\bar{\beta}-\bar{\gamma} = 0). \end{cases} \tag{4}$$

Interval(ii): $\dot{x} \leqslant 0,\ z \leqslant 0$

$$z = \begin{cases} -\dfrac{A - B_2 e^{(\bar{\beta}+\bar{\gamma})x}}{\bar{\beta}+\bar{\gamma}} & (\bar{\beta}+\bar{\gamma} \neq 0), \\ Ax + D_2 & (\bar{\beta}+\bar{\gamma} = 0). \end{cases} \tag{5}$$

Interval(iii): $\dot{x} \geqslant 0,\ z \leqslant 0$

$$z = \begin{cases} \dfrac{A - B_3 e^{-(\bar{\beta}-\bar{\gamma})x}}{\bar{\beta}-\bar{\gamma}} & (\bar{\beta}-\bar{\gamma} \neq 0), \\ Ax + D_3 & (\bar{\beta}-\bar{\gamma} = 0). \end{cases} \tag{6}$$

Interval(iv): $\dot{x} \geqslant 0,\ z \geqslant 0$

$$z = \begin{cases} \dfrac{A - B_4 e^{-(\bar{\beta}+\bar{\gamma})x}}{\bar{\beta}+\bar{\gamma}} & (\bar{\beta}+\bar{\gamma} \neq 0), \\ Ax + D_4 & (\bar{\beta}+\bar{\gamma} = 0), \end{cases} \tag{7}$$

where B_i and D_i are the constants of integration. Hysteretic restoring force z can be expressed in terms of the exponential functions of displacement x when $\bar{\beta} \pm \bar{\gamma} \neq 0$.

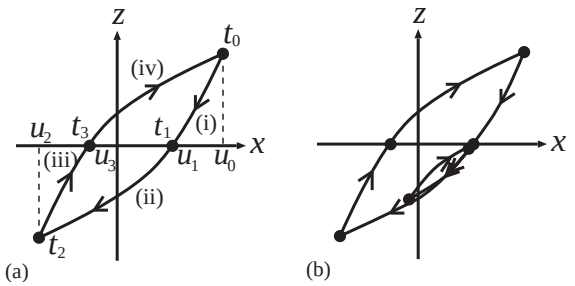

Fig. 1. Division of hysteretic loop: (a) single loop; (b) double loop.

3.2. The piecewise power series expression

We assume that the non-linearity of the restoring force is weak. Introducing small positive scaling parameter ε, the parameters $\bar{\beta}$ and $\bar{\gamma}$ which control non-linearity of hysteretic loop are replaced by $\varepsilon\beta$ and $\varepsilon\gamma$, respectively. Let $t_0, \ldots, t_3$ denote the time for each division point and let $u_0, \ldots, u_3$ denote the displacements at those points as shown in Fig. 1(a). For the hysteretic restoring force z to be continuous, the following conditions should be satisfied:

(1) When $t = t_0$ and $x = u_0$, $z(\mathrm{i}) = z(\mathrm{iv})$:

$$\frac{A - B_1 e^{\varepsilon(\beta-\gamma)u_0}}{\varepsilon(\beta-\gamma)} + \frac{A - B_4 e^{-\varepsilon(\beta+\gamma)u_0}}{\varepsilon(\beta+\gamma)} = 0. \tag{8}$$

(2) When $t = t_1$ and $x = u_1$, $z(\mathrm{i}) = z(\mathrm{ii}) = 0$:

$$A - B_1 e^{\varepsilon(\beta-\gamma)u_1} = 0, \quad A - B_2 e^{\varepsilon(\beta+\gamma)u_1} = 0. \tag{9}$$

(3) When $t = t_2$ and $x = u_2$, $z(\mathrm{ii}) = z(\mathrm{iii})$:

$$\frac{A - B_2 e^{\varepsilon(\beta+\gamma)u_2}}{\varepsilon(\beta+\gamma)} + \frac{A - B_3 e^{-\varepsilon(\beta-\gamma)u_2}}{\varepsilon(\beta-\gamma)} = 0. \tag{10}$$

(4) When $t = t_3$ and $x = u_3$, $z(\mathrm{iii}) = z(\mathrm{iv}) = 0$:

$$A - B_3 e^{-\varepsilon(\beta-\gamma)u_3} = 0, \quad A - B_4 e^{-\varepsilon(\beta+\gamma)u_3} = 0. \tag{11}$$

In these equations, z(i) to z(iv) denote z of intervals (i) to (iv), respectively.

By expanding $B_1, \ldots, B_4$ and the exponential functions in Eqs. (8)–(11) into power series of ε and equating coefficients of $\varepsilon^0, \varepsilon^1$ and ε^2, hysteretic restoring force is denoted by

$$z = A\left(x - \frac{u_0 + u_2}{2}\right) + \varepsilon z_1 + \varepsilon^2 z_2 + O(\varepsilon^3), \tag{12}$$

where z_1 and z_2 are the coefficients of order ε and ε^2, respectively. Let z_1 and z_2 in intervals (i), …, (iv) be $z_{11}, \ldots, z_{14}$ and $z_{21}, \ldots, z_{24}$, respectively. Their expressions are as follows:

$$z_{11} = \frac{A}{8}\{(\beta-\gamma)(u_0+u_2)^2 - \beta(u_0-u_2)^2 - 4(\beta-\gamma)(u_0+u_2)x + 4(\beta-\gamma)x^2\}, \tag{13}$$

$$z_{12} = \frac{A}{8}\{(\beta+\gamma)(u_0+u_2)^2 - \beta(u_0-u_2)^2 - 4(\beta+\gamma)(u_0+u_2)x + 4(\beta+\gamma)x^2\}, \tag{14}$$

$$z_{13} = -\frac{A}{8}\{(\beta-\gamma)(u_0+u_2)^2 - \beta(u_0-u_2)^2 - 4(\beta-\gamma)(u_0+u_2)x + 4(\beta-\gamma)x^2\}, \tag{15}$$

$$z_{14} = -\frac{A}{8}\{(\beta+\gamma)(u_0+u_2)^2 - \beta(u_0-u_2)^2 - 4(\beta+\gamma)(u_0+u_2)x + 4(\beta+\gamma)x^2\}, \tag{16}$$

$$z_{21} = \frac{A}{48}\{(2\beta^2-\gamma^2)(u_0+u_2)^3 + 6\beta\gamma u_0(u_0+u_2)^2 - 12\beta^2 u_0 u_2(u_0+u_2) - 8\beta\gamma u_0^3\}$$
$$-\frac{A}{8}(\beta-\gamma)\{\beta(u_0-u_2)^2 - (\beta-\gamma)(u_0+u_2)^2\}x$$
$$-\frac{A}{4}(\beta-\gamma)^2(u_0+u_2)x^2 + \frac{A}{6}(\beta-\gamma)^2x^3, \tag{17}$$

$$z_{22} = \frac{A}{48}\{(2\beta^2-\gamma^2)(u_0+u_2)^3 - 6\beta\gamma u_2(u_0+u_2)^2 - 12\beta^2 u_0 u_2(u_0+u_2) + 8\beta\gamma u_2^3\}$$
$$-\frac{A}{8}(\beta+\gamma)\{\beta(u_0-u_2)^2 - (\beta+\gamma)(u_0+u_2)^2\}x$$
$$-\frac{A}{4}(\beta+\gamma)^2(u_0+u_2)x^2 + \frac{A}{6}(\beta+\gamma)^2x^3, \tag{18}$$

$$z_{23} = \frac{A}{48}\{(2\beta^2-\gamma^2)(u_0+u_2)^3 + 6\beta\gamma u_2(u_0+u_2)^2 - 12\beta^2 u_0 u_2(u_0+u_2) - 8\beta\gamma u_2^3\}$$
$$-\frac{A}{8}(\beta-\gamma)\{\beta(u_0-u_2)^2 - (\beta-\gamma)(u_0+u_2)^2\}x$$
$$-\frac{A}{4}(\beta-\gamma)^2(u_0+u_2)x^2 + \frac{A}{6}(\beta-\gamma)^2x^3, \tag{19}$$

$$z_{24} = \frac{A}{48}\{(2\beta^2-\gamma^2)(u_0+u_2)^3 - 6\beta\gamma u_0(u_0+u_2)^2 - 12\beta^2 u_0 u_2(u_0+u_2) + 8\beta\gamma u_0^3\}$$
$$-\frac{A}{8}(\beta+\gamma)\{\beta(u_0-u_2)^2 - (\beta+\gamma)(u_0+u_2)^2\}x$$
$$-\frac{A}{4}(\beta+\gamma)^2(u_0+u_2)x^2 + \frac{A}{6}(\beta+\gamma)^2x^3. \tag{20}$$

At the time for each division point, $t_0, \ldots, t_3$, the following relations are satisfied:

$$u_0 = x(t_0), \tag{21}$$

$$u_1 = x(t_1) = \frac{u_0+u_2}{2} + \varepsilon\frac{\beta}{8}(u_0-u_2)^2 + O(\varepsilon^2), \tag{22}$$

$$u_2 = x(t_2), \tag{23}$$

$$u_3 = x(t_3) = \frac{u_0+u_2}{2} - \varepsilon\frac{\beta}{8}(u_0-u_2)^2 + O(\varepsilon^2). \tag{24}$$

Eqs. (12)–(24) can be parameterized by u_0 and u_2 instead of u_1 and u_3 so that hysteretic restoring force in steady state can be determined by the maximum and minimum of the displacement of the periodic solution. Even if $\bar{\beta} \pm \bar{\gamma} = 0$, that is, z cannot be described in terms of exponential function, Eqs. (12)–(24) are valid. It is noted that the parameters which correspond to softening characteristics in Wen's differential equation may correspond to hardening characteristics in the piecewise power series expression when the amplitude of response becomes large because of the approximation of exponential functions with polynomials.

Using the piecewise power series expression, the equation of motion for the present system is of the form

$$\ddot{x} + \bar{\delta}\dot{x} + (k + A)x - \frac{A}{2}(u_0 + u_2) + \varepsilon z_1 + \varepsilon^2 z_2 + O(\varepsilon^2) = \bar{f}\cos\omega t. \tag{25}$$

The linear natural frequency of this system is given by $\sqrt{k + A}$.

4. Multiple time scale analysis

We next apply the method of multiple time scales to the present system (25) up to the second order for the cases of primary and secondary resonance to obtain symmetric solutions and their stability. It is noted that in this analysis, not only the solution but also the restoring force are approximated due to the use of the piecewise power series expression.

4.1. Primary resonance

4.1.1. Expansion of the equation of motion

Introducing multiple time scales

$$T_n = \varepsilon^n t, \quad n = 0, 1, 2, \ldots, \tag{26}$$

The time derivative can be expressed as the following:

$$\frac{\mathrm{d}}{\mathrm{d}t} = D_0 + \varepsilon D_1 + \varepsilon^2 D_2 + \cdots, \tag{27}$$

$$\frac{\mathrm{d}^2}{\mathrm{d}t^2} = D_0^2 + 2\varepsilon D_0 D_1 + \varepsilon^2 (D_1^2 + 2D_0 D_2) + \cdots, \tag{28}$$

where $D_n = \partial/\partial T_n$.

We expand the displacement x and its maximum u_0 into the power series of ε since u_0 is unknown and determined by $x(t_0)$.

$$x = x_0 + \varepsilon x_1 + \varepsilon^2 x_2 + \cdots, \tag{29}$$

$$u_0 = u_{00} + \varepsilon u_{01} + \varepsilon^2 u_{02} + \cdots, \tag{30}$$

where x_i and u_{0i}, $i = 0, 1, 2$, are the terms of $O(\varepsilon^i)$. Since the steady state response in the primary resonance region can be assumed to be periodic and symmetric, i.e., $x(t) = -x(t + \pi/\omega), \dot{x}(t) = -\dot{x}(t + \pi/\omega)$ for any t, the maximum and minimum of the displacement satisfy the relation

$$u_0 = -u_2. \tag{31}$$

Moreover, we assume that the damping coefficient and the forcing amplitude is small and introduce a detuning parameter σ for the primary resonance region as

$$\bar{\delta} = \varepsilon\delta, \quad \bar{f} = \varepsilon f, \quad k + A - \omega^2 = \varepsilon\sigma. \tag{32}$$

Substituting Eqs. (27)–(32) into Eq. (25) and equating the coefficient of like powers of ε, the following differential equations are obtained:

$$\varepsilon^0\colon\ D_0^2 x_0 + \omega^2 x_0 = 0, \tag{33}$$

$$\varepsilon^1\colon\ D_0^2 x_1 + \omega^2 x_1 = -\sigma x_0 - \delta D_0 x_0 - 2D_0 D_1 x_0 - z_1' + f\cos\omega T_0, \tag{34}$$

$$\varepsilon^2\colon\ D_0^2 x_2 + \omega^2 x_2 = -\sigma x_1 - \delta(D_1 x_0 + D_0 x_1) - D_1^2 x_0 - 2D_0 D_2 x_0 - 2D_0 D_1 x_1 - z_2', \tag{35}$$

where z_1' and z_2' denote the coefficients of order ε and ε^2, respectively, in the expression of z which is obtained by substituting Eqs. (29)–(31) and (13)–(20) into Eq. (12) and re-expanding z to the power series of ε. The expressions of z_1' and z_2' are shown in Appendix A.

4.1.2. First order approximation

The solution of Eq. (33) is

$$x_0 = a(T_1, T_2, \ldots)\cos\{\omega T_0 + \theta(T_1, T_2, \ldots)\}, \tag{36}$$

where a and θ are the amplitude and phase of the solution. Substituting Eq. (36) into Eq. (34) yields

$$D_0^2 x_1 + \omega^2 x_1 = R_1(T_0) - z_1', \tag{37}$$

where

$$\begin{aligned} R_1(T_0) = &-\sigma a\cos(\omega T_0 + \theta) + \delta\omega a\sin(\omega T_0 + \theta) + f\cos\omega T_0 \\ &+ 2\omega\sin(\omega T_0 + \theta)D_1 a + 2\omega a\cos(\omega T_0 + \theta)D_1\theta. \end{aligned} \tag{38}$$

To eliminate the terms that produce secular terms, we determine the components of $\cos\omega T_0$ and $\sin\omega T_0$ of the right-hand side of Eq. (37) and equate them to zero. The condition for the component of $\cos\omega T_0$ to vanish is evaluated by

$$\int_{t_0}^{t_0+\frac{2\pi}{\omega}} \{R_1(T_0) - z_1'\}\cos\omega T_0\,\mathrm{d}T_0 = \sum_{i=1}^{4}\ \int_{t_{i-1}}^{t_i} \{R_1(T_0) - z_{1i}'\}\cos\omega T_0\,\mathrm{d}T_0, \tag{39}$$

where $t_4 = t_0 + 2\pi/\omega$.

To carry out the above integration, the times for each division point, $t_0, \ldots, t_3$ are necessary. From Eqs. (36), (22), (24) and (31), the displacements at each time are

$$\begin{aligned} &x(t_0) = a + O(\varepsilon), \quad x(t_1) = 0 + O(\varepsilon), \\ &x(t_2) = -a + O(\varepsilon), \quad x(t_3) = 0 + O(\varepsilon), \end{aligned} \tag{40}$$

so that we approximately set $t_0, \ldots, t_3$ as the following:

$$t_0 = -\frac{\theta}{\omega}, \quad t_1 = \frac{\pi}{2\omega} - \frac{\theta}{\omega}, \quad t_2 = \frac{\pi}{\omega} - \frac{\theta}{\omega}, \quad t_3 = \frac{3\pi}{2\omega} - \frac{\theta}{\omega}. \tag{41}$$

Calculating Eq. (39) by using Eq. (41) yields

$$f - \sigma a\cos\theta + \frac{4A\gamma a^2\cos\theta}{3\pi} + \frac{4A\beta a^2\sin\theta}{\pi} + \delta\omega a\sin\theta + 2\omega\sin\theta D_1 a + 2\omega a\cos\theta D_1\theta = 0, \tag{42}$$

where the relation $u_{00} = a$ derived from Eq. (40) was used.

Similarly, the condition for the coefficient of $\sin\omega T_0$ to vanish is

$$\delta\omega a\cos\theta + \frac{4A\beta a^2\cos\theta}{3\pi} + \sigma a\sin\theta - \frac{4A\gamma a^2\sin\theta}{3\pi} + 2\omega\cos\theta D_1 a - 2\omega a\sin\theta D_1\theta = 0. \tag{43}$$

Obtaining $D_1 a$ and $D_1\theta$ by solving Eqs. (42) and (43) yields a system of first order differential equations describing the modulation of the amplitude and phase of the response as follows:

$$\dot{a} = \varepsilon D_1 a = -\varepsilon\left(\frac{\delta a}{2} + \frac{f\sin\theta}{2\omega} + \frac{2a^2 A\beta}{3\omega\pi}\right), \tag{44}$$

$$\dot{\theta} = \varepsilon D_1\theta = \varepsilon\left(\frac{\sigma}{2\omega} - \frac{f\cos\theta}{2a\omega} - \frac{2aA\gamma}{3\omega\pi}\right). \tag{45}$$

The amplitude and phase of the first order approximate solution correspond to the fixed point of this system of differential equations. The stability of the solutions are determined by analyzing the behavior of Eqs. (44) and (45) in the neighborhood of the fixed points.

4.1.3. Second order approximation

We next derive the second order approximate solution $x_0 + \varepsilon x_1$.

Substituting $D_1 a$ and $D_1\theta$ described with Eqs. (44) and (45) into Eq. (37) and eliminating secular terms yield

$$D_0^2 x_1 + \omega^2 x_1 = -\frac{4A\gamma a^2\cos(\omega T_0 + \theta)}{3\pi} - \frac{4A\beta a^2\sin(\omega T_0 + \theta)}{3\pi} - z_1'. \tag{46}$$

Eq. (46) can be regarded as the undamped linear vibration equation with piecewise periodic external force, since z_1' on the right hand is defined in a piecewise manner. Although Eq. (46) apparently has secular terms with frequency ω, the terms are cancelled out by z_1' of four intervals as a whole. x_1 can be obtained by solving Eq. (46) for each interval so that the constants of integration satisfy the following conditions:

(1) The displacements and velocities of the four solutions are continuous,

$$x_{11}(t_1) = x_{12}(t_1), \quad x_{12}(t_2) = x_{13}(t_2), \quad x_{13}(t_3) = x_{14}(t_3), \tag{47}$$

$$\dot{x}_{11}(t_1) = \dot{x}_{12}(t_1), \quad \dot{x}_{12}(t_2) = \dot{x}_{13}(t_2), \quad \dot{x}_{13}(t_3) = \dot{x}_{14}(t_3), \tag{48}$$

where x_{1i}, $i = 1, \ldots, 4$, denote x_1 in interval i.

(2) The components of frequency ω in one period of x_1 vanish, i.e.,

$$\int_{t_0}^{t_0+2\pi/\omega} x_1\cos\omega T_0\,\mathrm{d}T_0 = 0, \quad \int_{t_0}^{t_0+2\pi/\omega} x_1\sin\omega T_0\,\mathrm{d}T_0 = 0. \tag{49}$$

Evaluating these conditions yields x_1 as in Appendix B.

We next derive a system of second order differential equations governing the amplitude and phase of the response.

To eliminate the secular terms, substituting Eqs. (36), (44), (45) and (B.1)–(B.4) into Eq. (35) and equating the coefficients of $\cos\omega T_0$ and $\sin\omega T_0$ zero yields

$$\begin{aligned}&\frac{3a^3A\beta^2\cos\theta}{8}-\delta D_1a\cos\theta-D_1^2a\cos\theta+aD_1\theta^2\cos\theta-\frac{a^3A\gamma^2\cos\theta}{8}\\&-\frac{7a^3A^2\beta^2\cos\theta}{24\omega^2}+\frac{5a^3A^2\gamma^2\cos\theta}{24\omega^2}+2aD_2\theta\omega\cos\theta+\frac{76a^3A^2\beta^2\cos\theta}{27\omega^2\pi^2}\\&-\frac{56a^3A^2\gamma^2\cos\theta}{27\omega^2\pi^2}+aD_1^2\theta\sin\theta+a\delta D_1\theta\sin\theta+2D_1aD_1\theta\sin\theta\\&+2D_2a\omega\sin\theta+\frac{4aA\beta u_{01}\sin\theta}{\pi}=0,\end{aligned}\tag{50}$$

$$\begin{aligned}&aD_1^2\theta\cos\theta+a\delta D_1\theta\cos\theta+2D_1aD_1\theta\cos\theta+2D_2a\omega\cos\theta+\frac{4aA\beta u_{01}\cos\theta}{\pi}\\&-\frac{3a^3A\beta^2\sin\theta}{8}+\delta D_1a\sin\theta+D_1^2a\sin\theta-aD_1\theta^2\sin\theta+\frac{a^3A\gamma^2\sin\theta}{8}\\&+\frac{7a^3A^2\beta^2\sin\theta}{24\omega^2}-\frac{5a^3A^2\gamma^2\sin\theta}{24\omega^2}-2aD_2\theta\omega\sin\theta-\frac{76a^3A^2\beta^2\sin\theta}{27\omega^2\pi^2}\\&+\frac{56a^3A^2\gamma^2\sin\theta}{27\omega^2\pi^2}=0.\end{aligned}\tag{51}$$

The expressions of D_1^2a, $D_1^2\theta$ and u_{01} in these equations need to be evaluated. D_1^2a and $D_1^2\theta$ are obtained by differentiating D_1a and $D_1\theta$ with T_1 using Eqs. (44) and (45) and expressed as

$$\begin{aligned}D_1^2a=&\frac{\delta^2a}{4}+\frac{8a^3A^2\beta^2}{9\omega^2\pi^2}+\frac{a^2A\beta\delta}{\omega\pi}+\frac{aAf\gamma\cos\theta}{3\omega^2\pi}\\&-\frac{f\sigma\cos\theta}{4\omega^2}+\frac{f^2\cos\theta^2}{4a\omega^2}+\frac{\delta f\sin\theta}{4\omega}+\frac{2aA\beta f\sin\theta}{3\omega^2\pi},\end{aligned}\tag{52}$$

$$D_1^2\theta=\frac{4a^2A^2\beta\gamma}{9\omega^2\pi^2}+\frac{aA\delta\gamma}{3\omega\pi}-\frac{\delta f\cos\theta}{4a\omega}-\frac{A\beta f\cos\theta}{3\omega^2\pi}+\frac{f\sigma\sin\theta}{4a\omega^2}-\frac{f^2\sin2\theta}{4a^2\omega^2}.\tag{53}$$

To obtain u_{01}, $x(t_0)$ is calculated by using Eqs. (40), (41) and (B.1).

$$x(t_0)=x_0(t_0)+\varepsilon x_{11}(t_0)+O(\varepsilon^2)=a-\varepsilon\frac{10-3\pi}{18\omega^3\pi}a^2A\gamma+O(\varepsilon^2).$$

Therefore,

$$u_{01}=-\frac{10-3\pi}{18\omega^3\pi}a^2A\gamma.\tag{54}$$

By solving D_2a and $D_2\theta$ from Eqs. (50) and (51) using Eqs. (44), (45), (52), (53) and (54), a system of second order differential equations describing the modulation of the amplitude a and

phase θ of the response is obtained as follows:

$$\begin{aligned}\dot{a} &= \varepsilon D_1 a + \varepsilon^2 D_2 a \\ &= -\varepsilon\left(\frac{\delta a}{2} + \frac{f\sin\theta}{2\omega} + \frac{2a^2 A\beta}{3\omega\pi}\right) \\ &\quad + \varepsilon^2\left(\frac{4a^3A^2\beta\gamma}{9\omega^3\pi^2} - \frac{a^3A^2\beta\gamma}{3\omega^3\pi} - \frac{a^2A\delta\gamma}{6\omega^2\pi} + \frac{a^2A\beta\sigma}{3\omega^3\pi}\right. \\ &\quad \left. + \frac{\delta f\cos\theta}{8\omega^2} - \frac{aA\beta f\cos\theta}{6\omega^3\pi} - \frac{aAf\gamma\sin\theta}{3\omega^3\pi} + \frac{f\sigma\sin\theta}{8\omega^3}\right),\end{aligned} \tag{55}$$

$$\begin{aligned}\dot{\theta} &= \varepsilon D_1\theta + \varepsilon^2 D_2\theta \\ &= \varepsilon\left(\frac{\sigma}{2\omega} - \frac{f\cos\theta}{2a\omega} - \frac{2aA\gamma}{3\omega\pi}\right) \\ &\quad + \varepsilon^2\left(\frac{7a^2A^2\beta^2}{48\omega^3} - \frac{5a^2A^2\gamma^2}{48\omega^3} - \frac{3a^2A\beta^2}{16\omega} - \frac{\delta^2}{8\omega} + \frac{a^2A\gamma^2}{16\omega}\right. \\ &\quad - \frac{26a^2A^2\beta^2}{27\omega^3\pi^2} + \frac{22a^2A^2\gamma^2}{27\omega^3\pi^2} + \frac{aA\beta\delta}{6\omega^2\pi} + \frac{aA\gamma\sigma}{3\omega^3\pi} - \frac{\sigma^2}{8\omega^3} \\ &\quad \left. - \frac{Af\gamma\cos\theta}{6\omega^3\pi} + \frac{f\sigma\cos\theta}{8a\omega^3} - \frac{\delta f\sin\theta}{8a\omega^2} + \frac{A\beta f\sin\theta}{3\omega^3\pi}\right).\end{aligned} \tag{56}$$

4.1.4. Stability analysis

The real parts of the eigenvalues of Jacobian matrix M_1 about the steady state solution of Eqs. (44) and (45) determine the stability of the first order approximate solution so that the solution is stable if $\mathrm{tr}(M_1)<0$ and $\det(M_1)>0$. Similarly, the stability of the second order approximate solution can be determined by Eqs. (55) and (56). It is confirmed that saddle-node bifurcation occurs in the primary resonance region as shown in Section 5.1.2.

4.2. Secondary resonance

Following almost the same procedure as for primary resonance, we obtain an approximate symmetric solution and a system of differential equations describing the modulation of amplitude of second order superharmonic component of the response.

4.2.1. Expansion of the equation of motion

For the case of secondary resonance, the displacement x and its maximum u_0 and minimum u_2 are expanded into the power series:

$$x = x_0 + \varepsilon x_1 + \varepsilon^2 x_2 + \cdots, \tag{57}$$

$$u_0 = u_{00} + \varepsilon u_{01} + \varepsilon^2 u_{02} + \cdots, \tag{58}$$

$$u_2 = u_{20} + \varepsilon u_{21} + \varepsilon^2 u_{22} + \cdots, \tag{59}$$

where x_i, u_{0i} and $u_{2i}, i = 0, 1, 2$ are the terms of $O(\varepsilon^i)$.

We assume that damping coefficient is small and introduce a detuning parameter σ. External forcing is not assumed to be small for the case of secondary resonance.

$$\bar{\delta} = \varepsilon\delta, \quad k + A = 4\omega^2 + \varepsilon\sigma, \quad \bar{f} = f. \tag{60}$$

Substituting Eqs. (27), (28), (57)–(60) into Eq. (25) and equating coefficients of like powers of ε, we obtain

$$\varepsilon^0\text{: } D_0^2 x_0 + 4\omega^2 x_0 = \frac{A}{2}(u_{00} + u_{20}) + f\cos\omega T_0, \tag{61}$$

$$\varepsilon^1\text{: } D_0^2 x_1 + 4\omega^2 x_1 = \frac{A}{2}(u_{01} + u_{21}) - \sigma x_0 - \delta D_0 x_0 - 2D_0 D_1 x_0 - z_1', \tag{62}$$

$$\varepsilon^2\text{: } D_0^2 x_2 + 4\omega^2 x_2 = \frac{A}{2}(u_{02} + u_{22}) - \sigma x_1 - D_1^2 x_0 - \delta(D_1 x_0 + D_0 x_1) - 2D_0 D_2 x_0 - 2D_0 D_1 x_1 - z_2', \tag{63}$$

where z_1' and z_2' denote the coefficients of order ε and ε^2, respectively, in the expression of z which is obtained by substituting Eqs. (57)–(59) into Eq. (25) and re-expanding z to the power series of ε. The expressions of z_1' and z_2' are shown in Appendix C.

4.2.2. First order approximation

The solution of Eq. (61) is

$$x_0 = a\cos 2\omega T_0 + b\sin 2\omega T_0 + \frac{f\cos\omega T_0}{3\omega^2} + \frac{A}{8\omega^2}(u_{00} + u_{20}), \tag{64}$$

where a and b are the amplitudes of the superharmonic component with frequency 2ω.

Hereafter, we consider the case that the solution is almost symmetric so that $a \approx b \approx 0$ and $u_{00} + u_{20} \approx 0$. Then the times for each division point are approximated as the following:

$$t_0 = 0, \quad t_1 = \frac{\pi}{2\omega}, \quad t_2 = \frac{\pi}{\omega}, \quad t_3 = \frac{3\pi}{2\omega}. \tag{65}$$

It is noted that Eq. (65) do not include arbitrary phase as opposed to Eq. (41) for primary resonance because the zeroth order solution (36) for primary resonance corresponds to free vibration while Eq. (64) is the response of forced vibration without damping.

By solving $u_{00} = x_0(t_0)$ and $u_{20} = x_0(t_2)$, u_{00} and u_{20} are obtained as

$$u_{00} = \frac{\bar{f}}{3\omega^2} - \frac{4\omega^2 a}{A - 4\omega^2}, \tag{66}$$

$$u_{20} = -\frac{\bar{f}}{3\omega^2} - \frac{4\omega^2 a}{A - 4\omega^2}. \tag{67}$$

Substituting Eqs. (66) and (67) into Eq. (64) yields the first order approximate solution,

$$x_0 = a\cos 2\omega T_0 + b\sin 2\omega T_0 + \frac{\bar{f}\cos\omega T_0}{3\omega^2} - \frac{Aa}{A - 4\omega^2}. \tag{68}$$

Substituting Eq. (64) into Eq. (62) and eliminating the coefficients of $\cos 2\omega T_0$ and $\sin 2\omega T_0$ yield a system of differential equations describing the modulation of amplitudes of superharmonic component of the response for the first order approximation:

$$\dot{a} = \varepsilon D_1 a = -\varepsilon\left(\frac{\delta a}{2} - \frac{\sigma b}{4\omega} + \frac{8A\beta\bar{f}a}{45\omega^3\pi} + \frac{8A\gamma\bar{f}b}{45\omega^3\pi}\right), \tag{69}$$

$$\dot{b} = \varepsilon D_1 b = -\varepsilon\left(\frac{\delta b}{2} + \frac{\sigma a}{4\omega} + \frac{2A\beta\bar{f}b}{45\omega^3\pi} - \frac{2A\bar{f}\gamma a}{45\omega^3\pi}\right). \tag{70}$$

4.2.3. Second order approximation

Substituting Eqs. (66)–(70) into Eq. (62) yields

$$\begin{aligned} D_0^2 x_1 + 4\omega^2 x_1 = & -\frac{\bar{f}\sigma}{3\omega^2}\cos\omega T_0 + \frac{\delta\bar{f}}{3\omega}\sin\omega T_0 + \frac{A\sigma a}{A-4\omega^2} + \frac{8A\bar{f}}{45\omega^2\pi}(\beta b - \gamma a)\cos 2\omega T_0 \\ & - \frac{32A\bar{f}}{45\omega^2\pi}(\beta a + \gamma b)\sin 2\omega T_0 + \frac{A}{2}(u_{01} + u_{21}) - z_1'. \end{aligned} \tag{71}$$

x_1 can be obtained in the piecewise manner using the same procedure as described in Section 4.1.3. Moreover, by solving the following two equations, u_{01} and u_{21} are obtained:

$$u_{01} = x_{11}(t_0), \quad u_{21} = x_{13}(t_2), \tag{72}$$

where $x_{11}(t_0)$ and $x_{13}(t_2)$ are the functions of u_{01} and u_{21}. It is noted that the times for each division point, $t_0, \ldots, t_3$, Eq. (65) are used in the above procedure.

Substitute $x_{11}, \ldots, x_{14}$ obtained above into Eq. (35) and evaluate the condition to make the secular terms vanish. By solving $D_2 a, D_2 b$ from the condition and using Eqs. (69) and (70), a system of differential equations governing the amplitudes of second order superharmonic component of the response for the second order approximation are derived as follows:

$$\begin{aligned} \dot{a} = & -\varepsilon\left(\frac{\delta a}{2} - \frac{\sigma b}{4\omega} + \frac{8A\beta\bar{f}a}{45\omega^3\pi} + \frac{8A\gamma\bar{f}b}{45\omega^3\pi}\right) \\ & + \varepsilon^2\left(\frac{-67A^2\beta\bar{f}^2\gamma a}{6075\omega^7\pi^2} + \frac{13A^2\beta\bar{f}^2\gamma a}{1620\omega^7\pi} - \frac{A\beta\bar{f}^2\gamma a}{54\omega^5\pi} + \frac{4A\delta\bar{f}\gamma a}{45\omega^4\pi} + \frac{79A\beta\bar{f}\sigma a}{1080\omega^5\pi}\right. \\ & - \frac{A^2\beta\gamma a^3}{3\omega^3\pi} + \frac{2A\beta\gamma a^3}{3\omega\pi} + \frac{17A^2\beta^2\bar{f}^2 b}{8640\omega^7} - \frac{11A^2\bar{f}^2\gamma^2 b}{2880\omega^7} - \frac{A\beta^2\bar{f}^2 b}{144\omega^5} + \frac{A\bar{f}^2\gamma^2 b}{144\omega^5} \\ & - \frac{\delta^2 b}{16\omega} + \frac{193A^2\beta^2\bar{f}^2 b}{10125\omega^7\pi^2} + \frac{244A^2\bar{f}^2\gamma^2 b}{30375\omega^7\pi^2} + \frac{8A\beta\delta\bar{f}b}{135\omega^4\pi} + \frac{79A\bar{f}\gamma\sigma b}{1080\omega^5\pi} - \frac{\sigma^2 b}{64\omega^3} \\ & - \frac{35A^2\beta^2 a^2 b}{384\omega^3} - \frac{35A^2\gamma^2 a^2 b}{384\omega^3} + \frac{5A\beta^2 a^2 b}{32\omega} + \frac{5A\gamma^2 a^2 b}{32\omega} - \frac{A^2\beta\gamma a b^2}{3\omega^3\pi} \\ & \left. + \frac{2A\beta\gamma a b^2}{3\omega\pi} - \frac{5A^2\beta^2 b^3}{384\omega^3} - \frac{5A^2\gamma^2 b^3}{384\omega^3} + \frac{A\beta^2 b^3}{32\omega} + \frac{A\gamma^2 b^3}{32\omega}\right), \end{aligned} \tag{73}$$

$$\begin{aligned}\dot{b} = &-\varepsilon\left(\frac{\delta b}{2}+\frac{\sigma a}{4\omega}+\frac{2A\beta\bar{f}b}{45\omega^3\pi}-\frac{2A\bar{f}\gamma a}{45\omega^3\pi}\right)\\ &+\varepsilon^2\left(\frac{-253A^2\beta^2\bar{f}^2a}{34560\omega^7}-\frac{31A^2\bar{f}^2\gamma^2a}{11520\omega^7}+\frac{A\beta^2\bar{f}^2a}{72\omega^5}+\frac{\delta^2a}{16\omega}+\frac{796A^2\beta^2\bar{f}^2a}{30375\omega^7\pi^2}\right.\\ &+\frac{29A^2\bar{f}^2\gamma^2a}{3375\omega^7\pi^2}+\frac{4A^2\bar{f}^2\gamma^2a}{405\omega^7\pi}-\frac{4A\beta\delta\bar{f}a}{45\omega^4\pi}-\frac{31A\bar{f}\gamma\sigma a}{1080\omega^5\pi}+\frac{\sigma^2a}{64\omega^3}+\frac{35A^2\beta^2a^3}{384\omega^3}\\ &-\frac{13A^2\gamma^2a^3}{384\omega^3}-\frac{5A\beta^2a^3}{32\omega}-\frac{5A\gamma^2a^3}{32\omega}+\frac{107A^2\beta\bar{f}^2\gamma b}{6075\omega^7\pi^2}-\frac{17A^2\beta\bar{f}^2\gamma b}{1620\omega^7\pi}\\ &+\frac{A\beta\bar{f}^2\gamma b}{54\omega^5\pi}-\frac{2A\delta\bar{f}\gamma b}{135\omega^4\pi}+\frac{31A\beta\bar{f}\sigma b}{1080\omega^5\pi}+\frac{A^2\beta\gamma a^2b}{6\omega^3\pi}-\frac{2A\beta\gamma a^2b}{3\omega\pi}+\frac{5A^2\beta^2ab^2}{384\omega^3}\\ &\left.+\frac{5A^2\gamma^2ab^2}{384\omega^3}-\frac{A\beta^2ab^2}{32\omega}-\frac{A\gamma^2ab^2}{32\omega}\right).\end{aligned} \tag{74}$$

It is noted that Eqs. (69) and (70) for the first order approximation and Eqs. (73) and (74) for the second order approximation have trivial steady state solution, $(a,b)=(0,0)$, which corresponds to symmetric solutions. By substituting the solution $(a,b)=(0,0)$ into Eq. (68) and $x_{11},\ldots,x_{14}$, the second order symmetric approximate solution is obtained as Appendix D.

4.2.4. Stability analysis

In the above analysis, the instability of the trivial solution $(a,b)=(0,0)$ corresponds to the divergence of a non-symmetric solution. We next evaluate the unstable parameter regions of the trivial solution for the first order and the second order approximation.

Jacobian matrix M_1 about the steady state solution $(a,b)=(0,0)$ of Eqs. (69) and (70) is derived as

$$M_1=\varepsilon\begin{pmatrix}-\dfrac{\delta}{2}-\dfrac{8A\beta\bar{f}}{45\omega^3\pi} & \dfrac{\sigma}{4\omega}-\dfrac{8A\gamma\bar{f}}{45\omega^3\pi}\\ -\dfrac{\sigma}{4\omega}+\dfrac{2A\gamma\bar{f}}{45\omega^3\pi} & -\dfrac{\delta}{2}-\dfrac{2A\beta\bar{f}}{45\omega^3\pi}\end{pmatrix}. \tag{75}$$

Since $\mathrm{tr}(M_1)<0$, $\det(M_1)=0$ gives the stability limit outside which the symmetric solution becomes unstable. It can be confirmed that the equilibrium point $(a,b)=(0,0)$ changes from stable node to saddle point by crossing the limit for the first order approximation. By arranging $\det(M_1)>0$, the condition that the symmetric solution becomes unstable and non-symmetric solution diverges when $\bar{\delta}=0$ can be derived as the next inequality:

$$4\bar{\beta}<3|\bar{\gamma}|. \tag{76}$$

Similarly, for the second order approximation, the stability limit outside which the non-symmetric solution diverges is given by $\det(M_2)=0$ and $\mathrm{tr}(M_2)<0$, where M_2 is Jacobian matrix of steady state solution $(a,b)=(0,0)$. We can confirm that this condition corresponds to pitchfork bifurcation [19,20] for the second order approximation.

Although there exists the possibility of another bifurcation when $\mathrm{tr}(M_2)=0$, $\det(M_2)>0$, it is beyond the scope of this paper.

Tedious computations required in this section were performed by using *Mathematica* [23].

5. Comparison with numerical integration

In order to examine the validity of the present analysis, we carry out the numerical integration of Eq. (3) and compare the results with those of the multiple time scale analysis. We set $A = 0.95$ and $k = 0.05$ to consider the case that the hysteretic restoring force is predominant over the linear one, and set the damping coefficient $\bar{\delta} = 0.1$ and the amplitude of excitation $\bar{f} = 0.5$ for the weak damping and excitation. The linear natural frequency of the system is $\sqrt{k + A} = 1.0$.

5.1. Primary resonance

5.1.1. Phase plane trajectories

Fig. 2 shows the phase plane trajectories, where (a) and (b) are for the case of softening hysteresis, while (c) and (d) are for the case of hardening hysteresis. The solid and dashed lines represent, respectively, the second order and the first order approximate solutions obtained by multiple time scale analysis. The dotted lines represent the numerical solutions of Eq. (3) obtained by shooting method [24].

The orbits of analytical solutions and numerical solutions are in similar tendency. A good agreement is found between the second order approximate solutions and the numerical ones. Although the second order approximate solutions are given in the piecewise manner, the phase

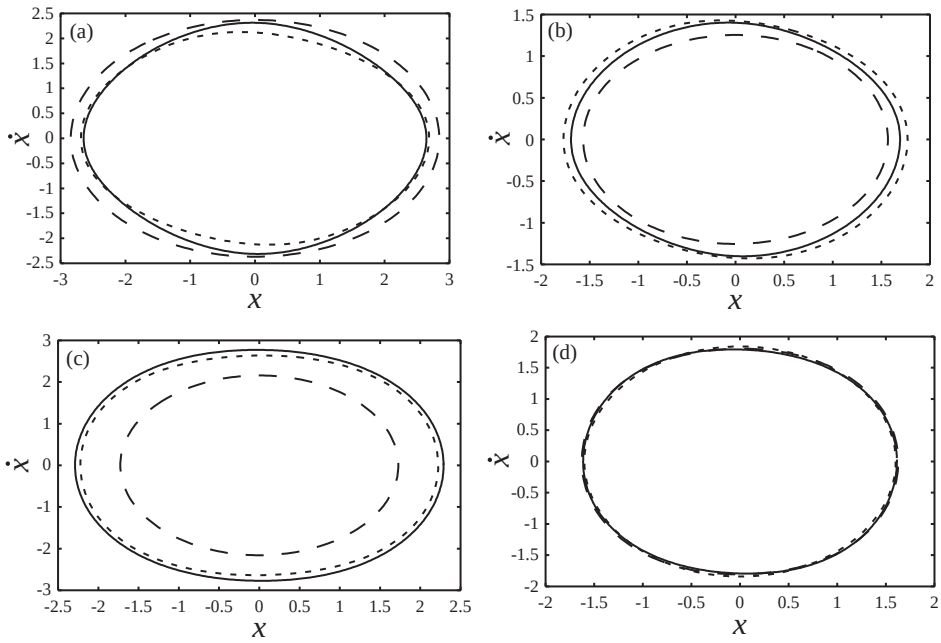

Fig. 2. Phase plane trajectories: (a) $\bar{\beta} = 0.1$, $\bar{\gamma} = 0.5$, $\omega = 0.8$ (softening); (b) $\bar{\beta} = 0.3$, $\bar{\gamma} = 0.3$, $\omega = 0.8$ (softening); (c) $\bar{\beta} = 0.1$, $\bar{\gamma} = -0.5$, $\omega = 1.25$ (hardening); (d) $\bar{\beta} = 0.3$, $\bar{\gamma} = -0.5$, $\omega = 1.15$ (hardening). In all cases, $A = 0.95$, $k = 0.05$, $\bar{\delta} = 0.1$ and $\bar{f} = 0.5$. ———, MS second order; — — —, MS first order; - - - -, numerical.

plane trajectories are continuous and smooth. This is because the piecewise expression for hysteretic restoring force is continuous at the times for each division point.

5.1.2. Resonance curves

Figs. 3 and 4 show the resonance curves of the softening and hardening hysteretic systems, respectively, for several values of $\bar{\beta}$ and $\bar{\gamma}$. The solid and dashed lines represent the results of the second order and the first order approximation, respectively, and the dotted lines represent those of numerical integration. The resonance curves obtained from the first and second order multiple time scale analyses are similar to the curves of numerical integration. It is noted that the second order approximate solutions show better agreement with the numerical integration than the first order ones.

5.2. Secondary resonance

5.2.1. Phase plane trajectories

Fig. 5 shows the phase plane trajectories of the second order approximate solution and the numerical integration for four parameter choices. The theoretical results are calculated by Eqs. (D.1)–(D.5), while the numerical results are calculated by numerical integration of Eq. (3).

Figs. 5(a) and (b) are for the case of softening hysteresis, while Figs. 5(c) and (d) are for the case of hardening hysteresis. The solid lines represent the second order approximate solutions and the

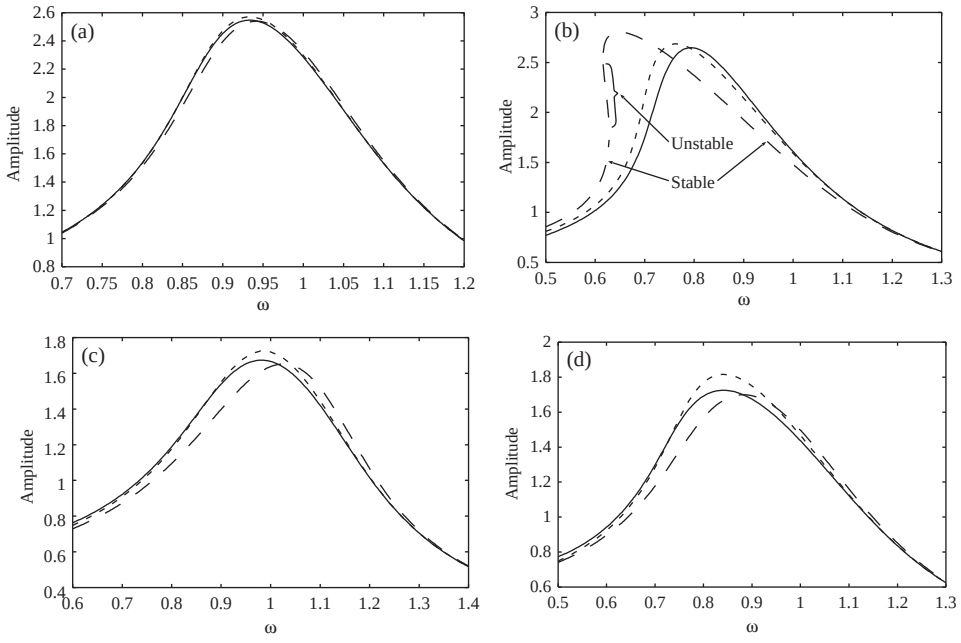

Fig. 3. Resonance curves for softening systems; (a) $\bar{\beta}=0.1$, $\bar{\gamma}=0.1$; (b) $\bar{\beta}=0.1$, $\bar{\gamma}=0.5$; (c) $\bar{\beta}=0.3$, $\bar{\gamma}=-0.1$; (d) $\bar{\beta}=0.3$, $\bar{\gamma}=0.3$. In all cases, $A=0.95$, $k=0.05$, $\bar{\delta}=0.1$ and $\bar{f}=0.5$. ———, MS second order; — — —, MS first order; - - - -, numerical.

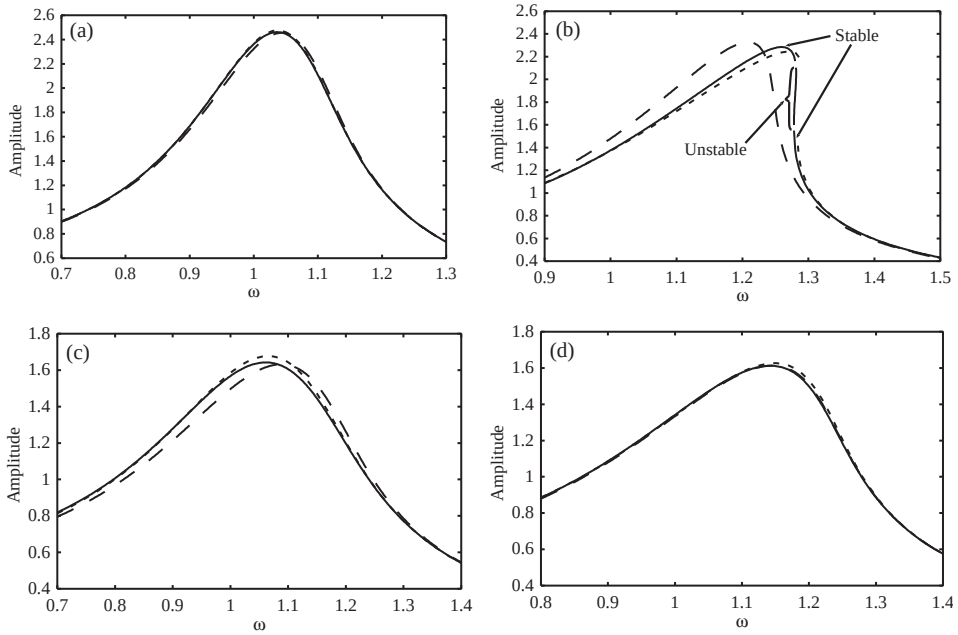

Fig. 4. Resonance curves for hardening systems; (a) $\bar{\beta} = 0.1$, $\bar{\gamma} = -0.1$; (b) $\bar{\beta} = 0.1$, $\bar{\gamma} = -0.5$; (c) $\bar{\beta} = 0.3$, $\bar{\gamma} = -0.3$; (d) $\bar{\beta} = 0.3$, $\bar{\gamma} = -0.5$. In all cases, $A = 0.95$, $k = 0.05$, $\bar{\delta} = 0.1$ and $\bar{f} = 0.5$. ———, MS second order; — — —, MS first order; - - - -, numerical.

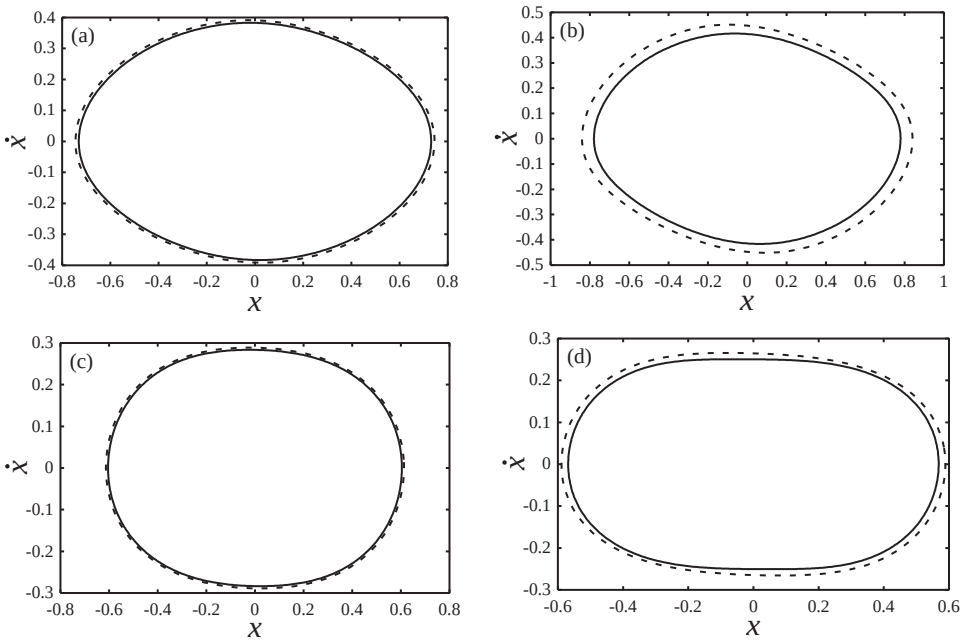

Fig. 5. Phase plane trajectories: (a) $\bar{\beta} = 0.1$, $\bar{\gamma} = 0.3$ (softening); (b) $\bar{\beta} = 0.3$, $\bar{\gamma} = 0.5$ (softening); (c) $\bar{\beta} = 0.1$, $\bar{\gamma} = -0.3$ (hardening); (d) $\bar{\beta} = 0.3$, $\bar{\gamma} = -0.5$ (hardening). In all cases, $\bar{f} = 0.5$, $\omega = 0.5$, $\bar{\delta} = 0$, $A = 0.95$ and $k = 0.05$. ———, MS second order; - - - -, numerical.

dashed lines represent the orbits of numerical integration. A fairly good agreement is found in both the results.

5.2.2. Divergence of non-symmetric solution

The resonance curve of a softening hysteretic system obtained by numerical integration of Eq. (3) is shown in Fig. 6 in order to explain how the symmetric solution bifurcates to non-symmetric solutions. Point P corresponds to the primary resonance and points Q and R correspond to the secondary resonance. Periodic solutions and hysteretic loops at the points P, Q and R are computed by the shooting method and are shown in Figs. 7(a), (b) and (c), respectively. While symmetric solution (Fig. 7(a)) is stable in the primary resonance region, symmetric solution (Fig. 7(b)) becomes unstable and stable non-symmetric solution (Fig. 7(c)) diverges in the secondary resonance region. The bifurcation diagram for the same hysteretic system is shown in Fig. 8. As ω increases or decreases, one symmetric solution becomes unstable and bifurcates to two non-symmetric solutions. The divergence of non-symmetric solution corresponds to pitchfork bifurcation, which qualitatively agrees with the stability analysis described in Section 4.2.4.

5.2.3. Unstable region of symmetric solution

Figs. 9 and 10 show the unstable regions of symmetric solutions for softening and hardening hysteretic systems, respectively. In each figure, $\bar{\beta}$ and $\bar{\gamma}$ are selected to satisfy condition (76). The solid and dashed lines represent the results of the second order and the first order approximation, respectively, and the dotted line represents the results of the numerical integration.

The unstable regions of symmetric solution diverge from point $(f,\omega)=(0,\sqrt{k+A}/2)$ and spread over to upper left regions in softening systems (Fig. 9(a)) and upper right regions in hardening systems (Fig. 10(a)). The regions become larger as non-linearity increases (Figs. 9(b) and 10(b)) and move up as damping coefficient δ increases (Figs. 9(c) and 10(c)).

The results of the first and second order approximations are qualitatively similar to those of numerical integration for all cases. Moreover, the second order approximate results are quantitatively closer to a numerical one than the first order results.

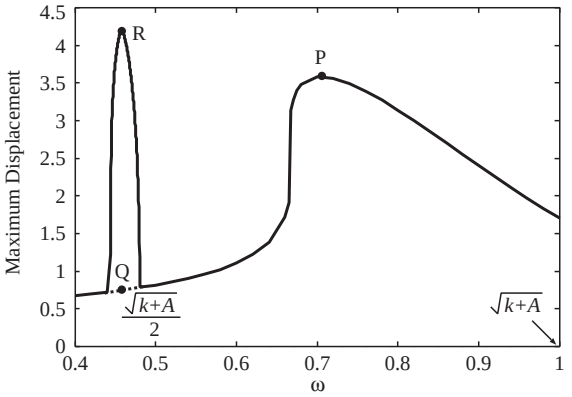

Fig. 6. Resonance curve of a softening hysteretic system: $\bar{\beta}=0.1$, $\bar{\gamma}=0.5$, $A=0.95$, $k=0.05$, $\bar{\delta}=0$ and $\bar{f}=0.5$. ———, stable; · · · · ·, unstable.

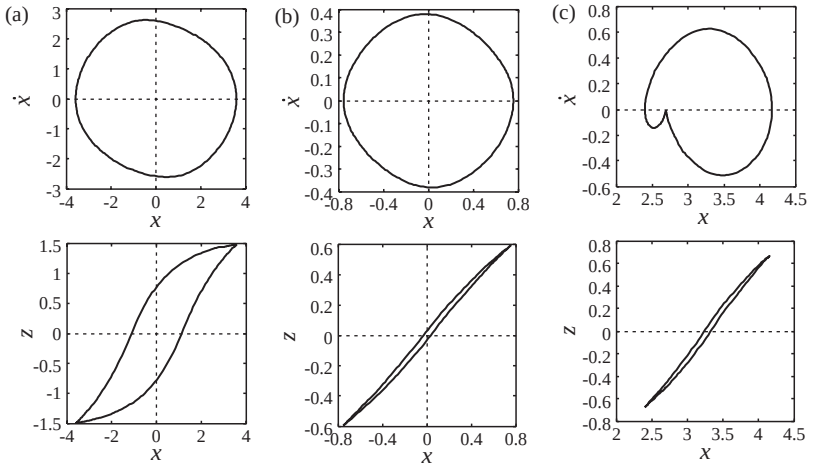

Fig. 7. Phase plane trajectories and hysteretic loops: (a) Stable symmetric solution (point P, $\omega = 0.7$); (b) Unstable symmetric solution (point Q, $\omega = 0.46$); (c) Stable non-symmetric solution (point R, $\omega = 0.46$). In all cases, $\bar{\beta} = 0.1$, $\bar{\gamma} = 0.5$, $A = 0.95$, $k = 0.05$, $\bar{\delta} = 0$ and $\bar{f} = 0.5$.

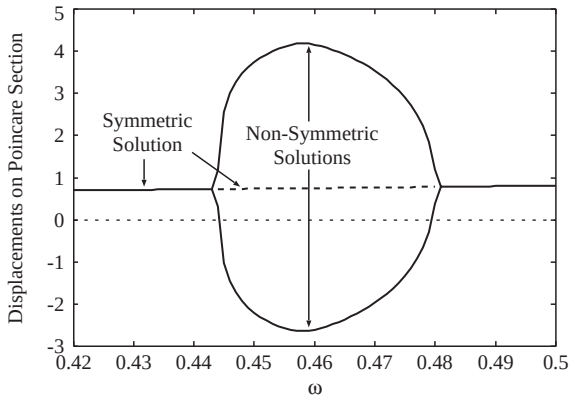

Fig. 8. Bifurcation diagram for a softening system: $\bar{\beta} = 0.1$, $\bar{\gamma} = 0.5$, $A = 0.95$, $k = 0.05$, $\bar{\delta} = 0$ and $\bar{f} = 0.5$. ———, stable; - - - - -, unstable.

6. Conclusions

A smooth hysteretic system subjected to harmonic excitation was analyzed. As a model for hysteresis, Wen's differential equation, which governs hysteretic restoring force by differential equation, was used. To apply the method of multiple time scales, the piecewise power series expression for hysteretic restoring force was proposed under the assumption that the non-linearity of the restoring force is weak and the force–displacement curve draws a single loop.

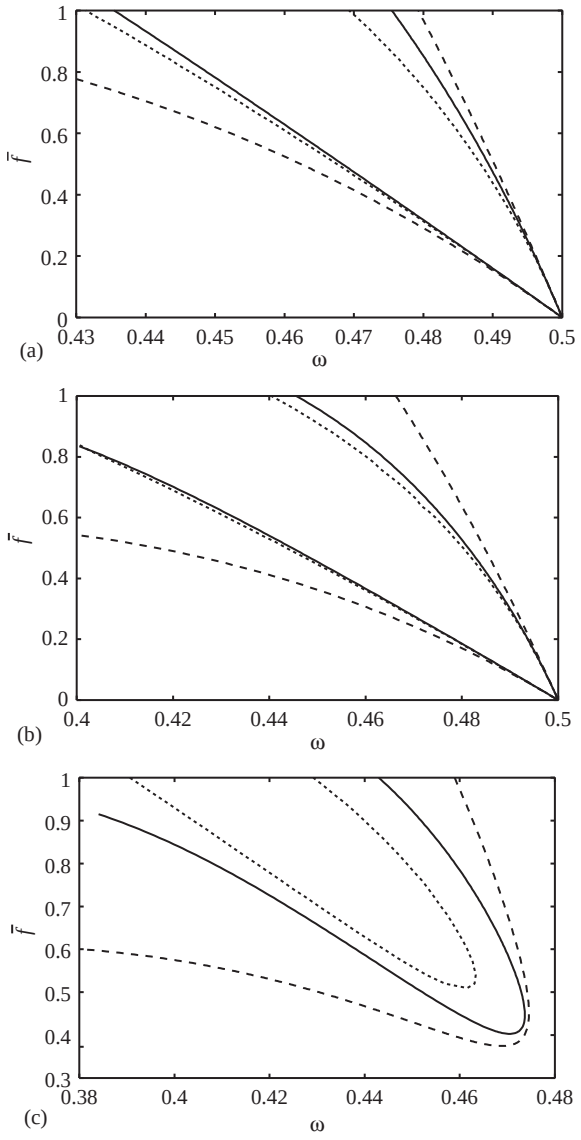

Fig. 9. Unstable regions of symmetric solutions for softening systems: (a) $\bar{\beta} = 0.1$, $\bar{\gamma} = 0.3$, $\bar{\delta} = 0$; (b) $\bar{\beta} = 0.1$, $\bar{\gamma} = 0.5$, $\bar{\delta} = 0$; (c) $\bar{\beta} = 0.1$, $\bar{\gamma} = 0.5$, $\bar{\delta} = 0.05$. In all cases, $A = 0.95$ and $k = 0.05$. ———, MS second order; – – – –, MS first order; · · · · ·, numerical.

By using the piecewise power series expression and the method of multiple time scales, the first and second order approximate solutions and the systems of differential equations describing the modulation of the amplitudes and phases of the solutions were obtained for the cases of primary and secondary resonance. Stability analysis for the solutions of the secondary resonance was also performed and the unstable regions of symmetric solutions were determined.

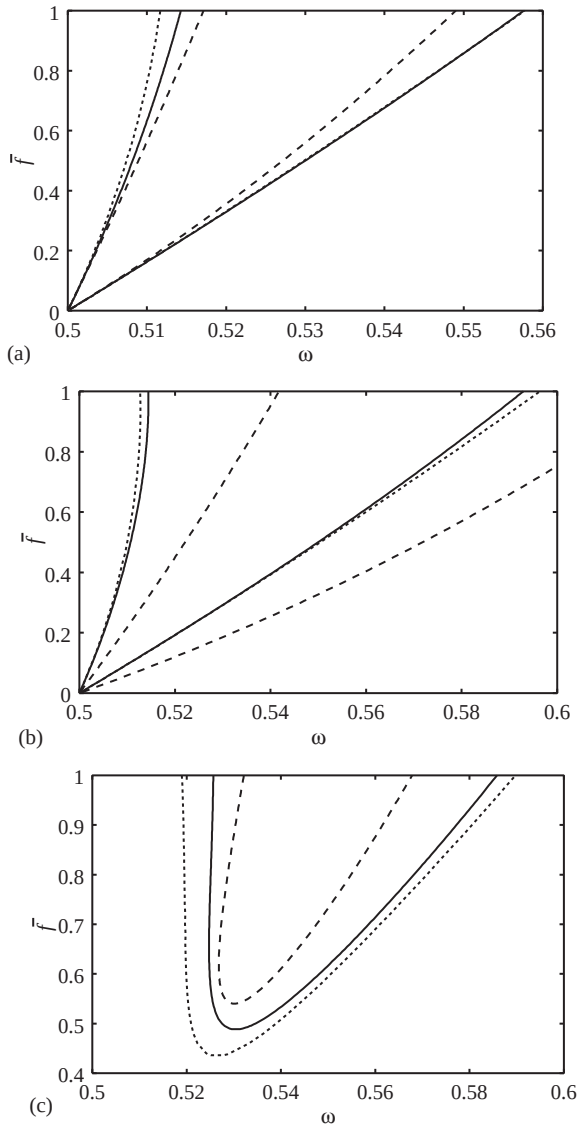

Fig. 10. Unstable regions of symmetric solutions for hardening systems: (a) $\bar{\beta} = 0.1$, $\bar{\gamma} = -0.3$, $\bar{\delta} = 0$; (b) $\bar{\beta} = 0.1$, $\bar{\gamma} = -0.5$, $\bar{\delta} = 0$; (c) $\bar{\beta} = 0.1$, $\bar{\gamma} = -0.5$, $\bar{\delta} = 0.05$. In all cases, $A = 0.95$ and $k = 0.05$. ———, MS second order; – – – –, MS first order; · · · · ·, numerical.

Phase plane trajectories, resonance curves and the unstable regions of symmetric solutions obtained from the analyses were compared with the results of numerical integration and the validity of the present method was confirmed.

The proposed method can be applied to a large class of hysteretic systems. Extending the method to the case of non-symmetric solution is the subject of further study in the future.

Appendix A

The expressions of $z'_{11}, \ldots, z'_{24}$ for the case of primary resonance are as follows:

$$z'_{11} = \frac{A}{2}\{(\beta-\gamma)x_0^2 - \beta u_{00}^2\}, \tag{A.1}$$

$$z'_{12} = \frac{A}{2}\{(\beta+\gamma)x_0^2 - \beta u_{00}^2\}, \tag{A.2}$$

$$z'_{13} = -\frac{A}{2}\{(\beta-\gamma)x_0^2 - \beta u_{00}^2\}, \tag{A.3}$$

$$z'_{14} = -\frac{A}{2}\{(\beta+\gamma)x_0^2 - \beta u_{00}^2\}, \tag{A.4}$$

$$z'_{21} = \frac{A}{6}\{(\beta-\gamma)^2x_0^3 - 3\beta(\beta-\gamma)u_{00}^2x_0 + 6(\beta-\gamma)x_0x_1 - \beta\gamma u_{00}^3 - 6\beta u_{00}u_{01}\}, \tag{A.5}$$

$$z'_{22} = \frac{A}{6}\{(\beta+\gamma)^2x_0^3 - 3\beta(\beta+\gamma)u_{00}^2x_0 + 6(\beta+\gamma)x_0x_1 - \beta\gamma u_{00}^3 - 6\beta u_{00}u_{01}\}, \tag{A.6}$$

$$z'_{23} = \frac{A}{6}\{(\beta-\gamma)^2x_0^3 - 3\beta(\beta-\gamma)u_{00}^2x_0 - 6(\beta-\gamma)x_0x_1 + \beta\gamma u_{00}^3 + 6\beta u_{00}u_{01}\}, \tag{A.7}$$

$$z'_{24} = \frac{A}{6}\{(\beta+\gamma)^2x_0^3 - 3\beta(\beta+\gamma)u_{00}^2x_0 - 6(\beta+\gamma)x_0x_1 + \beta\gamma u_{00}^3 + 6\beta u_{00}u_{01}\}. \tag{A.8}$$

Appendix B

The expressions of $x_{11}, \ldots, x_{14}$ for the case of primary resonance are as follows:

$$\begin{aligned} x_{11}(T_0) = {} & \frac{a^2A\beta}{4\omega^2} + \frac{a^2A\gamma}{4\omega^2} - \frac{a^2A\beta\cos(\omega T_0+\theta)}{3\omega^2} - \frac{5a^2A\gamma\cos(\omega T_0+\theta)}{9\omega^2\pi} \\ & + \frac{2a^2A\beta(\omega T_0+\theta)\cos(\omega T_0+\theta)}{3\omega^2\pi} + \frac{a^2A\beta\cos 2(\omega T_0+\theta)}{12\omega^2} \\ & - \frac{a^2A\gamma\cos 2(\omega T_0+\theta)}{12\omega^2} - \frac{5a^2A\beta\sin(\omega T_0+\theta)}{9\omega^2\pi} \\ & - \frac{2a^2A\gamma(\omega T_0+\theta)\sin(\omega T_0+\theta)}{3\omega^2\pi}, \end{aligned} \tag{B.1}$$

$$x_{12}(T_0) = \frac{a^2A\beta}{4\omega^2} - \frac{a^2A\gamma}{4\omega^2} - \frac{a^2A\beta\cos(\omega T_0+\theta)}{3\omega^2} - \frac{5a^2A\gamma\cos(\omega T_0+\theta)}{9\omega^2\pi} + \frac{2a^2A\beta(\omega T_0+\theta)\cos(\omega T_0+\theta)}{3\omega^2\pi} + \frac{a^2A\beta\cos 2(\omega T_0+\theta)}{12\omega^2} + \frac{a^2A\gamma\cos 2(\omega T_0+\theta)}{12\omega^2} + \frac{2a^2A\gamma\sin(\omega T_0+\theta)}{3\omega^2} - \frac{5a^2A\beta\sin(\omega T_0+\theta)}{9\omega^2\pi} - \frac{2a^2A\gamma(\omega T_0+\theta)\sin(\omega T_0+\theta)}{3\omega^2\pi}, \tag{B.2}$$

$$x_{13}(T_0) = -\frac{a^2A\beta}{4\omega^2} - \frac{a^2A\gamma}{4\omega^2} - \frac{a^2A\beta\cos(\omega T_0+\theta)}{\omega^2} - \frac{5a^2A\gamma\cos(\omega T_0+\theta)}{9\omega^2\pi} + \frac{2a^2A\beta(\omega T_0+\theta)\cos(\omega T_0+\theta)}{3\omega^2\pi} - \frac{a^2A\beta\cos 2(\omega T_0+\theta)}{12\omega^2} + \frac{a^2A\gamma\cos 2(\omega T_0+\theta)}{12\omega^2} + \frac{2a^2A\gamma\sin(\omega T_0+\theta)}{3\omega^2} - \frac{5a^2A\beta\sin(\omega T_0+\theta)}{9\omega^2\pi} - \frac{2a^2A\gamma(\omega T_0+\theta)\sin(\omega T_0+\theta)}{3\omega^2\pi}, \tag{B.3}$$

$$x_{14}(T_0) = -\frac{a^2A\beta}{4\omega^2} + \frac{a^2A\gamma}{4\omega^2} - \frac{a^2A\beta\cos(\omega T_0+\theta)}{\omega^2} - \frac{5a^2A\gamma\cos(\omega T_0+\theta)}{9\omega^2\pi} + \frac{2a^2A\beta(\omega T_0+\theta)\cos(\omega T_0+\theta)}{3\omega^2\pi} - \frac{a^2A\beta\cos 2(\omega T_0+\theta)}{12\omega^2} - \frac{a^2A\gamma\cos 2(\omega T_0+\theta)}{12\omega^2} + \frac{4a^2A\gamma\sin(\omega T_0+\theta)}{3\omega^2} - \frac{5a^2A\beta\sin(\omega T_0+\theta)}{9\omega^2\pi} - \frac{2a^2A\gamma(\omega T_0+\theta)\sin(\omega T_0+\theta)}{3\omega^2\pi}. \tag{B.4}$$

Appendix C

The expressions of $z'_{11}, \ldots, z'_{24}$ for the case of secondary resonance are the following:

$$z'_{11} = \frac{A}{8}\{-\beta(u_{00}-u_{20})^2 + (\beta-\gamma)(u_{00}+u_{20})^2 - 4(\beta-\gamma)(u_{00}+u_{20})x_0 + 4(\beta-\gamma)x_0^2\} - \frac{A}{2}(u_{01}+u_{21}), \tag{C.1}$$

$$z'_{12} = \frac{A}{8}\{-\beta(u_{00}-u_{20})^2 + (\beta+\gamma)(u_{00}+u_{20})^2 - 4(\beta+\gamma)(u_{00}+u_{20})x_0 + 4(\beta+\gamma)x_0^2\} - \frac{A}{2}(u_{01}+u_{21}), \tag{C.2}$$

$$z'_{13} = \frac{A}{8}\{\beta(u_{00}-u_{20})^2 - (\beta-\gamma)(u_{00}+u_{20})^2 + 4(\beta-\gamma)(u_{00}+u_{20})x_0 - 4(\beta-\gamma)x_0^2\} - \frac{A}{2}(u_{01}+u_{21}), \tag{C.3}$$

$$z'_{14} = \frac{A}{8}(\beta(u_{00}-u_{20})^2 - (\beta+\gamma)(u_{00}+u_{20})^2 + 4(\beta+\gamma)(u_{00}+u_{20})x_0 - 4(\beta+\gamma)x_0^2\} - \frac{A}{2}(u_{01}+u_{21}), \tag{C.4}$$

$$\begin{aligned} z'_{21} = {} & \frac{A}{48}\{-8\beta\gamma u_{00}^3 - 12\beta^2 u_{00}u_{20}(u_{00}+u_{20}) + 6\beta\gamma u_{00}(u_{00}+u_{20})^2 + (2\beta^2-\gamma^2)(u_{00}+u_{20})^3\} \\ & - \frac{A}{8}(\beta-\gamma)\{\beta(u_{00}-u_{20})^2 - (\beta-\gamma)(u_{00}+u_{20})^2\}x_0 \\ & - \frac{A}{4}(\beta-\gamma)^2(u_{00}+u_{20})x_0^2 + \frac{A}{6}(\beta-\gamma)^2x_0^3 \\ & + \frac{A}{8}[-2\beta(u_{00}-u_{20})(u_{01}-u_{21}) + 2(\beta-\gamma)(u_{00}+u_{20})(u_{01}+u_{21}) \\ & + 8(\beta-\gamma)x_0x_1 - 4(\beta-\gamma)\{(u_{01}+u_{21})x_0 + (u_{00}+u_{20})x_1\}] \\ & - \frac{A}{2}(u_{02}+u_{22}), \end{aligned} \tag{C.5}$$

$$\begin{aligned} z'_{22} = {} & \frac{A}{48}\{8\beta\gamma u_{20}^3 - 12\beta^2 u_{00}u_{20}(u_{00}+u_{20}) - 6\beta\gamma u_{20}(u_{00}+u_{20})^2 + (2\beta^2-\gamma^2)(u_{00}+u_{20})^3\} \\ & - \frac{A}{8}(\beta+\gamma)\{\beta(u_{00}-u_{20})^2 - (\beta+\gamma)(u_{00}+u_{20})^2\}x_0 \\ & - \frac{A}{4}(\beta+\gamma)^2(u_{00}+u_{20})x_0^2 + \frac{A}{6}(\beta+\gamma)^2x_0^3 \\ & + \frac{A}{8}[-2\beta(u_{00}-u_{20})(u_{01}-u_{21}) + 2(\beta+\gamma)(u_{00}+u_{20})(u_{01}+u_{21}) \\ & + 8(\beta+\gamma)x_0x_1 - 4(\beta+\gamma)\{(u_{01}+u_{21})x_0 + (u_{00}+u_{20})x_1\}] \\ & - \frac{A}{2}(u_{02}+u_{22}), \end{aligned} \tag{C.6}$$

$$\begin{aligned} z'_{23} = {} & \frac{A}{48}\{-8\beta\gamma u_{20}^3 - 12\beta^2 u_{00}u_{20}(u_{00}+u_{20}) + 6\beta\gamma u_{20}(u_{00}+u_{20})^2 + (2\beta^2-\gamma^2)(u_{00}+u_{20})^3\} \\ & - \frac{A}{8}(\beta-\gamma)\{\beta(u_{00}-u_{20})^2 - (\beta-\gamma)(u_{00}+u_{20})^2\}x_0 \\ & - \frac{A}{4}(\beta-\gamma)^2(u_{00}+u_{20})x_0^2 + \frac{A}{6}(\beta-\gamma)^2x_0^3 \end{aligned}$$

$$+\frac{A}{8}[2\beta(u_{00}-u_{20})(u_{01}-u_{21})-2(\beta-\gamma)(u_{00}+u_{20})(u_{01}+u_{21})$$
$$-8(\beta-\gamma)x_0x_1+4(\beta-\gamma)\{(u_{01}+u_{21})x_0+(u_{00}+u_{20})x_1\}]$$
$$-\frac{A}{2}(u_{02}+u_{22}), \tag{C.7}$$

$$z'_{24}=\frac{A}{48}\{8\beta\gamma u_{00}^3-12\beta^2u_{00}u_{20}(u_{00}+u_{20})-6\beta\gamma u_{00}(u_{00}+u_{20})^2+(2\beta^2-\gamma^2)(u_{00}+u_{20})^3\}$$
$$-\frac{A}{8}(\beta+\gamma)\{\beta(u_{00}-u_{20})^2-(\beta+\gamma)(u_{00}+u_{20})^2\}x_0$$
$$-\frac{A}{4}(\beta+\gamma)^2(u_{00}+u_{20})x_0^2+\frac{A}{6}(\beta+\gamma)^2x_0^3$$
$$+\frac{A}{8}[2\beta(u_{00}-u_{20})(u_{01}-u_{21})-2(\beta+\gamma)(u_{00}+u_{20})(u_{01}+u_{21})$$
$$-8(\beta+\gamma)x_0x_1+4(\beta+\gamma)\{(u_{01}+u_{21})x_0+(u_{00}+u_{20})x_1\}]$$
$$-\frac{A}{2}(u_{02}+u_{22}). \tag{C.8}$$

Appendix D

The second order symmetric approximate solution for the case of secondary resonance is expressed as follows:

$$x_0=\frac{\bar{f}}{3\omega^2}\cos\omega t, \tag{D.1}$$

$$x_{11}=\frac{A^2\beta\bar{f}^2}{144\omega^6(A-4\omega^2)}+\frac{A^2\bar{f}^2\gamma}{144\omega^6(A-4\omega^2)}-\frac{A\beta\bar{f}^2}{36\omega^4(A-4\omega^2)}$$
$$-\frac{A\bar{f}^2\gamma}{36\omega^4(A-4\omega^2)}-\frac{\bar{f}\sigma\cos\omega t}{9\omega^4}-\frac{A\beta\bar{f}^2\cos2\omega t}{144\omega^6}+\frac{A\bar{f}^2\gamma\cos2\omega t}{144\omega^6}$$
$$+\frac{\delta\bar{f}\sin\omega t}{9\omega^3}+\frac{A\beta\bar{f}^2\pi\sin2\omega t}{288\omega^6}-\frac{A\beta\bar{f}^2t\sin2\omega t}{144\omega^5}+\frac{A\bar{f}^2\gamma t\sin2\omega t}{144\omega^5}, \tag{D.2}$$

$$x_{12}=\frac{A^2\beta\bar{f}^2}{144\omega^6(A-4\omega^2)}+\frac{A\bar{f}^2\gamma}{36\omega^4(A-4\omega^2)}-\frac{A^2\bar{f}^2\gamma}{144\omega^6(A-4\omega^2)}$$
$$-\frac{A\beta\bar{f}^2}{36\omega^4(A-4\omega^2)}-\frac{\bar{f}\sigma\cos\omega t}{9\omega^4}-\frac{A\beta\bar{f}^2\cos2\omega t}{144\omega^6}-\frac{A\bar{f}^2\gamma\cos2\omega t}{144\omega^6}$$
$$+\frac{\delta\bar{f}\sin\omega t}{9\omega^3}+\frac{A\beta\bar{f}^2\pi\sin2\omega t}{288\omega^6}+\frac{A\bar{f}^2\gamma\pi\sin2\omega t}{144\omega^6}-\frac{A\beta\bar{f}^2t\sin2\omega t}{144\omega^5}$$
$$-\frac{A\bar{f}^2\gamma t\sin2\omega t}{144\omega^5}, \tag{D.3}$$

$$x_{13} = \frac{A\beta\bar{f}^2}{36\omega^4(A-4\omega^2)} + \frac{A\bar{f}^2\gamma}{36\omega^4(A-4\omega^2)} - \frac{A^2\beta\bar{f}^2}{144\omega^6(A-4\omega^2)} - \frac{A^2\bar{f}^2\gamma}{144\omega^6(A-4\omega^2)} - \frac{\bar{f}\sigma\cos\omega t}{9\omega^4} + \frac{A\beta\bar{f}^2\cos 2\omega t}{144\omega^6} - \frac{A\bar{f}^2\gamma\cos 2\omega t}{144\omega^6} + \frac{\delta\bar{f}\sin\omega t}{9\omega^3} - \frac{A\beta\bar{f}^2\pi\sin 2\omega t}{96\omega^6} + \frac{A\bar{f}^2\gamma\pi\sin 2\omega t}{144\omega^6} + \frac{A\beta\bar{f}^2 t\sin 2\omega t}{144\omega^5} - \frac{A\bar{f}^2\gamma t\sin 2\omega t}{144\omega^5}, \tag{D.4}$$

$$x_{14} = \frac{A^2\bar{f}^2\gamma}{144\omega^6(A-4\omega^2)} + \frac{A\beta\bar{f}^2}{36\omega^4(A-4\omega^2)} - \frac{A^2\beta\bar{f}^2}{144\omega^6(A-4\omega^2)} - \frac{A\bar{f}^2\gamma}{36\omega^4(A-4\omega^2)} - \frac{\bar{f}\sigma\cos\omega t}{9\omega^4} + \frac{A\beta\bar{f}^2\cos 2\omega t}{144\omega^6} + \frac{A\bar{f}^2\gamma\cos 2\omega t}{144\omega^6} + \frac{\delta\bar{f}\sin\omega t}{9\omega^3} - \frac{A\beta\bar{f}^2\pi\sin 2\omega t}{96\omega^6} - \frac{A\bar{f}^2\gamma\pi\sin 2\omega t}{72\omega^6} + \frac{A\beta\bar{f}^2 t\sin 2\omega t}{144\omega^5} + \frac{A\bar{f}^2\gamma t\sin 2\omega t}{144\omega^5}. \tag{D.5}$$

References

[1] R. Pratap, P. Holmes, Chaos in a mapping describing elastoplastic oscillations, *Nonlinear Dynamics* 8 (1995) 111–139.

[2] D. Capecchi, Periodic response and stability of hysteretic oscillators, *Dynamics and Stability of Systems* 6 (1991) 89–106.

[3] C.Y. Yang, A.H-D. Cheng, R.V. Roy, Chaotic and stochastic dynamics for a nonlinear structural system with hysteresis and degradation, *Probabilistic Engineering Mechanics, Part 2* 6 (1991) 193–203.

[4] T.K. Caughey, Sinusoidal excitation of a system with bilinear hysteresis, *Transactions of the American Society of Mechanical Engineers, Journal of Applied Mechanics* 27 (1960) 640–643.

[5] P.C. Jennings, Periodic response of a general yielding structure, *Proceedings of the American Society of Civil Engineers, Journal of Engineering Mechanics* 90 (1964) 131–166.

[6] D. Capecchi, F. Vestroni, Steady-state dynamic analysis of hysteretic systems, *Proceedings of the American Society of Civil Engineers, Journal of Engineering Mechanics* 111 (1985) 1515–1531.

[7] W.D. Iwan, D.M. Furuike, The transient and steady-state response of a hereditary system, *International Journal of Non-linear Mechanics* 8 (1973) 395–406.

[8] G.R. Miller, The steady-state response of systems with hardening hysteresis, *Transactions of the American Society of Mechanical Engineers, Journal of Mechanical Design* 100 (1978) 193–198.

[9] D. Capecchi, F. Vestroni, Periodic response of a class of hysteretic oscillators, *International Journal of Non-linear Mechanics* 25 (1990) 309–317.

[10] W.D. Iwan, The steady-state response of a two-degree-of-freedom bilinear hysteretic system, *Transactions of the American Society of Mechanical Engineers, Journal of Applied Mechanics* 32 (1965) 151–156.

[11] I.C. Jongs, On stability of a circulately system with bilinear hysteretic damping, *Transactions of the American Society of Mechanical Engineers, Journal of Applied Mechanics* 36 (1969) 76–82.

[12] C. Hayashi, *Nonlinear Oscillations in Physical Systems*, McGraw-Hill, New York, 1964.

[13] C.W. Wong, Y.Q. Ni, S.L. Lau, Steady-state oscillation of hysteretic differential model. I: response analysis, *Proceedings of the American Society of Civil Engineers, Journal of Engineering Mechanics* 120 (1994) 2271–2298.
[14] A.H. Nayfeh, Perturbation Method, Wiley-Interscience, New York, 1973.
[15] C. Holmes, P. Holmes, Second order averaging and bifurcations to subharmonics in duffing's equation, *Journal of Sound and Vibration* 78 (1981) 161–174.
[16] B. Poddar, F.C. Moon, S. Mukherjee, Chaotic motion of an elastic plastic beam, *Transactions of the American Society of Mechanical Engineers, Journal of Applied Mechanics* 55 (1988) 185–189.
[17] R. Pratap, S. Mukherjee, F.C. Moon, Dynamic behavior of a bilinear hysteretic elasto-plastic oscillator, Part I: free oscillations, *Journal of Sound and Vibration* 172 (1994) 321–337.
[18] R. Pratap, S. Mukherjee, F.C. Moon, Dynamic behavior of a bilinear hysteretic elasto-plastic oscillator, Part II: oscillations under periodic impulse forcing, *Journal of Sound and Vibration* 172 (1994) 339–358.
[19] J. Guckenheimer, P. Holmes, *Nonlinear Oscillations, Dynamical Systems, and Bifurcations of Vector Fields*, Springer, Berlin, 1983.
[20] S. Wiggins, *Introduction to Applied Nonlinear Dynamical Systems and Chaos*, Springer, Berlin, 1990.
[21] T.T. Baber, Y.K. Wen, Random vibration of hysteretic, degrading systems, *Proceedings of the American Society of Civil Engineers, Journal of Engineering Mechanics* 107 (1981) 1069–1087.
[22] Y.K. Wen, Method for random vibration of hysteretic systems, *Proceedings of the American Society of Civil Engineers, Journal of Engineering Mechanics* 102 (1976) 249–263.
[23] S. Wolfram, *Mathematica Second Edition*, Addison-Wesley, Reading, MA, 1992.
[24] T.S. Parker, L.O. Chua, *Practical Numerical Algorithms for Chaotic Systems*, Springer, Berlin, 1989.